

PRELIMINARY NUMERICAL MODELLING OF A PIPE-TO-TANK CONNECTIONS EXPERIMENTAL CAMPAIGN

Chiara Miglietta¹, Daniele Perrone¹, Giammaria Gabbianelli², Gianni Blasi¹, Francesco Micelli¹, and Mariano Ciucci³

¹ University of Salento
via per Monteroni Complesso Ecotekne, Lecce (Italy)
e-mail: {chiara.miglietta,daniele.perrone,gianni.blasi,francesco.micelli}@unisalento.it

² University of Pavia
via Ferrata, Pavia (Italy)
giammaria.gabbianelli@unipv.it

³ INAIL, Department of Technological Innovations and Safety of Plants
via del Torraccio di Torrenova, Roma (Italy)
m.ciucci@inail.it

Abstract

Damage occurred during past seismic events in industrial facilities pointed out the vulnerability of pipe-to-tank connections with the consequent loss of functionality of industrial plants as well as the release of hazardous substances. The observed damages are mainly due to the relative displacements between pipes and storage tanks because of their significant differences in terms of dynamic properties. In industrial facilities dealing with hazardous substances, even the smallest crack could release toxic containment, posing serious threats to both the environment and human lives. This highlights the need to further investigate the seismic response of pipe-to-tank connections to reduce the risk of major accidents following a seismic event. This paper presents and discusses the results of preliminary finite element models of pipe-to-tank connections under monotonic and cyclic loading in three different loading conditions. The models are developed to predict the experimental hysteretic responses of pipe-to-tank connections that will be tested as part of an experimental campaign carried out at the University of Salento in the framework of the MITPLANT project funded by National Institute for Insurance against Accidents at Work. Once validated through the experimental results, the numerical models will be useful for investigating the seismic vulnerability of complex piping networks in industrial facilities as well as for optimising the design of possible retrofit solutions.

Keywords: Damage, Pipe-to-tank connection, Earthquake, FE-models

1 INTRODUCTION

The seismic vulnerability assessment of industrial plants and their components is essential for preserving their structural integrity and ensuring the safety of both the environment and human life during a seismic event. Earthquakes and other natural events could cause technological disasters; for this reason, they are among the so-called “Natech events” (Natural Hazard Triggering Technological Disasters) [1]. The consequences of these extreme events could be catastrophic, especially when plants and tanks store hazardous substances. In addition to possible structural damage, the leakage of toxic substances could cause fires or explosions, leading to environmental damage and loss of life. Financial damage could also occur due to a temporary interruption in the plant's serviceability.

The seismic vulnerability of industrial plants has been clearly demonstrated in past seismic events, evidenced by the damage to supporting structures, complex piping networks, and large storage tanks [2, 3]. Understanding and mitigating these risks is crucial for ensuring safety and preventing costly disruptions [4]. Focusing on steel tank damage involves several failure modes, including elephant's foot buckling, roof damage [5], base plate deformation, anchor bolt failure, and nozzle damage [6], as reported in Figure 1.

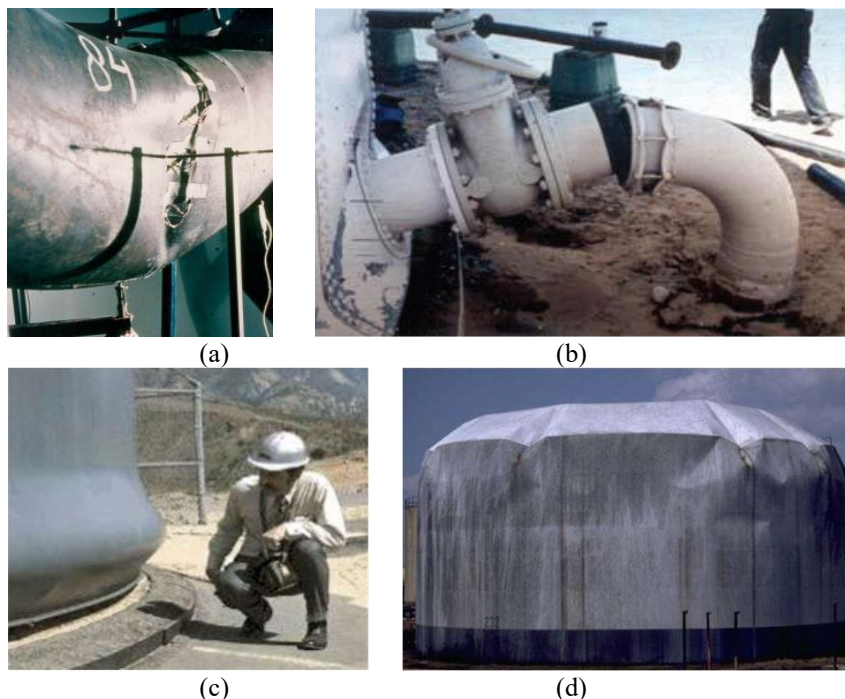


Figure 1: (a) effect of local buckling in a pipe [6], (b) failure of pipe-to-tank connection [18], (c) elephant's foot buckling [6], (d) roof damage [6]

To improve the seismic performance of steel tank, EN 1998-4 “Eurocode 8: Design of structures for earthquake resistance – Part 4: Silos, tanks and pipelines” and EN 14015 “Specification for the design and manufacture of site built, vertical, cylindrical, flat-bottomed, above ground, welded, steel tanks for the storage liquids at ambient temperature and above” [7, 8] provide design and analysis criteria. Among the American codes, those developed by the American Petroleum Institute may be useful for tanks design and analysis, namely API 650 “Welded Tanks for Oil Storage” and API 620 “Design and Construction of Large, Welded, Low-pressure Storage Tanks” [9, 10, 11] are of particular interest. However, for a complete understanding of the dynamic response of steel tanks integrated within complex piping networks further investigations are still required.

To this aim, the present work, developed within the MITPLANT (Mitigation of seismic vulnerability for industrial plants at relevant risk) research project founded by INAIL (Italian National Institute for Insurance against Accidents at Work), focuses on the characterization of the hysteretic response of pipe-to-tank connections in order to provide performance parameters useful in the design process.

An extensive experimental campaign has been designed to characterise the response of pipe-to-tank connections subjected to monotonic and cyclic loadings in different directions. To design the experimental campaign and predict the expected response, advanced preliminary numerical models have been developed. This step is crucial for optimizing the setup configuration and properly selecting the actuator to be used during the experimental tests. In this paper, the experimental campaign is described, with a focus on the results of the preliminary numerical analyses. Once further calibrated based on the test results, these models will be used for conducting parametric analyses and will serve as a valuable tool for practitioners evaluating the performance of complex piping networks in industrial facilities.

2 DESCRIPTION OF THE EXPERIMENTAL CAMPAIGN

Some components in industrial plants, such as elbows, pipe-to-pipe and pipe-to-tank connections, can be characterized by a quite complex non-linear behaviour. Therefore, conducting experimental tests can be beneficial in evaluating their seismic response and predicting potential damage modes.

For example, among pipe-to-pipe connections, Reza et al. [12] designed non-standard bolted flange joints and evaluated their performance through several monotonic and cyclic tests under pure bending and axial loading. This experimental campaign was extended by La Sallandra et al. [13], with monotonic and cyclic tests of the same non-standard bolted flanged joints under combined axial and shear loading. Varelis et al. [14] examined the behaviour of pipe elbows under cyclic in-plane bending loading and in presence of internal pressure, while Papatheocharis et al. [15] focused on the performance of Tee pipe junctions under strong cyclic loading.

Aiba et al. [16] conducted experimental tests on nozzles installed at sidewall of a reduced-scale cylindrical tank. Wieschollek et al. [17] described the results of six experimental tests on three typical types of shell nozzle reinforcement; these monotonic and cyclic tests were carried out under longitudinal and transverse load directions to develop appropriate finite element models for parametrical numerical investigations.

In this context, experimental tests on pipe-to-tank connections under different loading conditions have been planned at the University of Salento in the framework of the MITPLANT Project funded by INAIL.

The experimental campaign aims to investigate the nonlinear cyclic response of pipe-to-tank connections under various loading conditions. Specifically, the specimens will be tested in axial, transverse, and combined loading directions, subjected to both monotonic and cyclic loading protocols. Each specimen consists of a perforated steel plate that simulates the region of the tank wall near the connection, with a steel pipe welded into the hole to represent the pipe attached to the tank. Materials and thickness of the specimens were selected according to EN 14015:2006 [8], which provides specifications for nozzle design. The materials' properties adopted in the experimental campaign are detailed in Table 1, while in Table 2 is reported the complete test matrix of the experimental program.

	Steel grade	Yield strength (N/mm ²)	Thickness (mm)	Dimension
Shell plate	S275JO	275	5	500x500 mm
Nozzle	P355N	355	8.5	DN100

Table 1: Materials and thicknesses of specimens.

Test ID	Specimen	Test protocol
#1	S1	Monotonic
#2	S1	Cyclic
#3	S1	Cyclic
#4	S2	Monotonic
#5	S2	Cyclic
#6	S2	Cyclic
#7	S3	Monotonic
#8	S3	Cyclic
#9	S3	Cyclic

Table 2: Description of experimental program

Since the universal testing machine applies the load in the longitudinal direction, three specific setups were designed in order to simulate the different loading conditions. Figure 2, Figure 3 and Figure 4 report the geometrical characteristics of the specimens, respectively named S1 for specimen tested in axial direction, S2 for transverse direction and S3 for the combined loading direction.

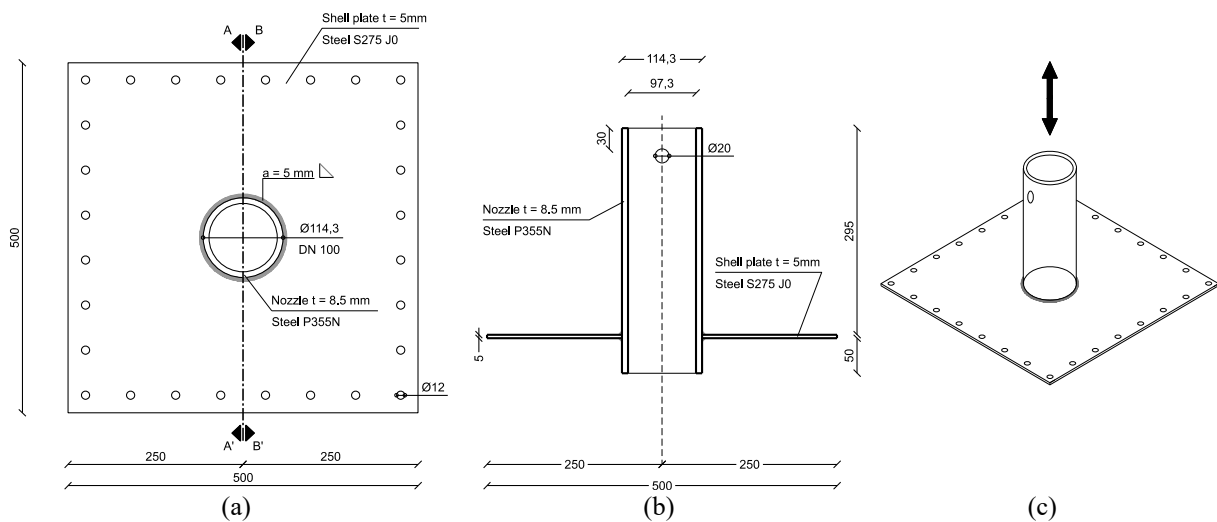


Figure 2: Characteristics of specimen S1: (a) front view, (b) section A-A', (c) 3D view

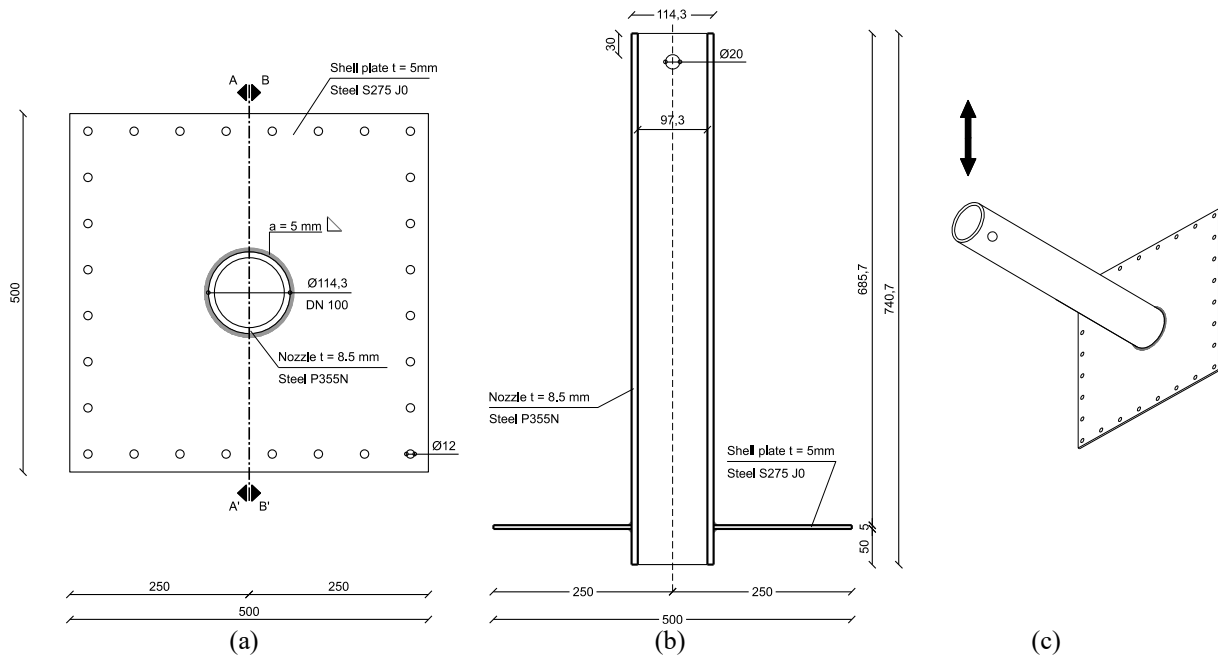


Figure 3: Characteristics of specimen S2: (a) front view, (b) section A-A', (c) 3D view

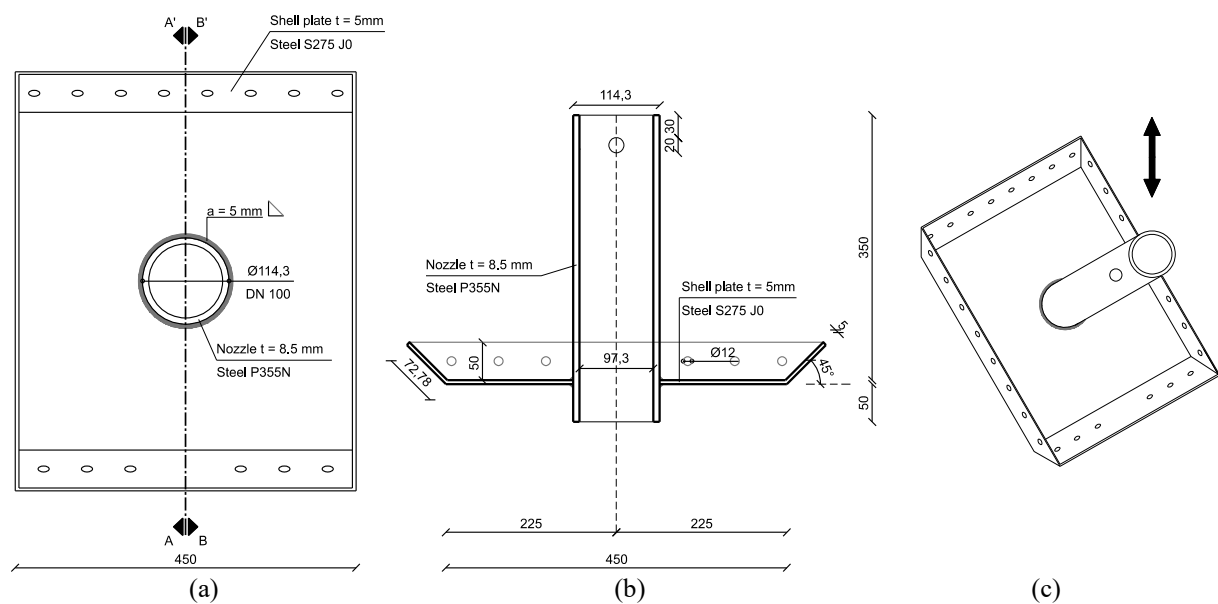


Figure 4: Characteristics of specimen S3: (a) front view, (b) section A-A', (c) 3D view

3 PRELIMINARY NUMERICAL MODELLING

Preliminary nonlinear static analyses were conducted to simulate the response of the three proposed configurations (S1, S2, and S3). The numerical models were developed using MIDAS FEA NX software. The study aims to predict the results of the experimental tests and to calibrate the loading protocols for cyclic testing, which will be further validated based on the results of the monotonic tests. The finite element models replicate the geometric dimensions (Figures 2-4) and material properties (Table 1) used in the specimen fabrication. Shell elements were employed in the numerical models, considering both geometric and material nonlinearity. An elastic perfectly-plastic behaviour was assumed for the steel material. Fixed boundary conditions were applied along the perimeter of the steel plate, assuming that the specimens will be rigidly bolted to the supports, simulating the extension of the tank's wall.

Figure 5 shows the resulting numerical models. Displacements were applied at the pipe end through a master node located at the centre of the steel pipe, which is connected by a rigid link to all nodes along the pipe's circumference.

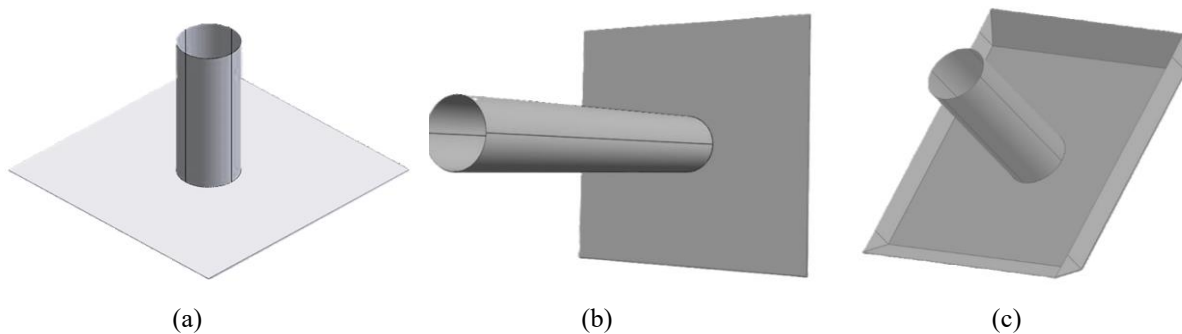


Figure 5: Finite element models: (a) S1, (b) S2, (c) S3

3.1 Numerical simulation of quasi-static monotonic tests

According to FEMA 461 [19], monotonic tests are required to define displacement amplitudes for cyclic testing. For this reason, and in order to investigate the effectiveness of the numerical models, monotonic nonlinear static analyses were performed. As shown in Figure 6, the increasing monotonic load was applied separately in two opposite directions for each specimen.

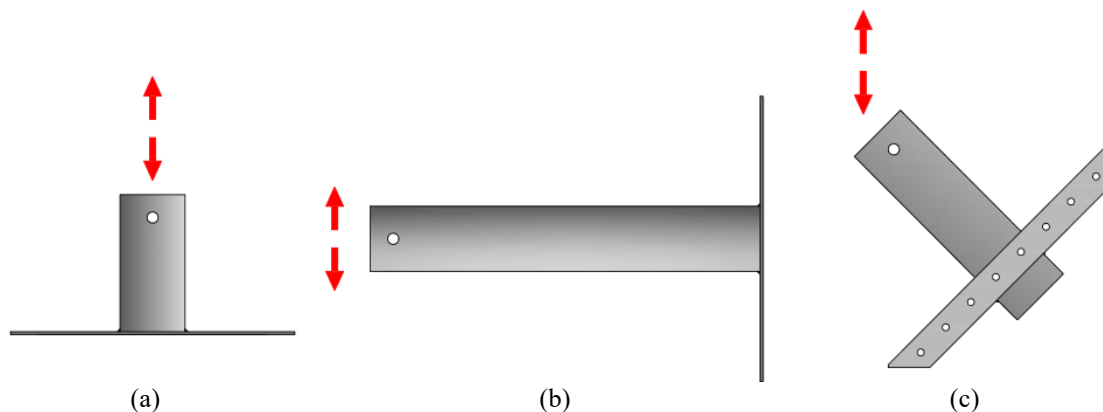


Figure 6: Load directions: (a) specimen 1 (S1), (b) specimen 2 (S2), (c) specimen 3 (S3)

The following plots present the results of nonlinear static analyses in terms of load-displacement curves.

Analysing the curves for S1 (Figure 7), an initial elastic response was observed up to a displacement of approximately 7.5 mm in compression and 10 mm in tension. As the displacement increased, plastic deformations were noted. During the compression loading analysis, the maximum force reached approximately 140 kN, followed by a degradation phase associated with specimen buckling. In contrast, a different response was observed when tensile displacement was applied: no degradation phase occurred, and both the steel plate and the pipe-to-plate connection progressively yielded up to the maximum displacement achieved during the analysis. These results indicate that compressive forces are more critical for the analysed configuration. The red dotted line in Figure 7 represents the target maximum deformation amplitude (Δ_m) adopted for the calibration of the quasi-static cyclic loading protocol.

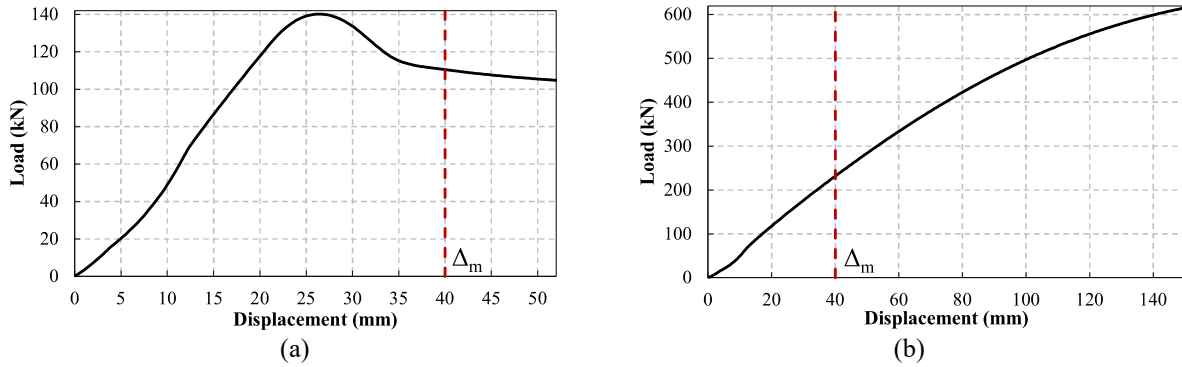


Figure 7: Monotonic load-displacement curves for S1: (a) compression, (b) tension

In the case of S2, the load-displacement curves exhibited a nearly identical trend in both loading directions (Figure 8). This behaviour can be attributed to the geometric symmetry of the specimen, as well as the symmetry of the applied constraints and loading conditions, which resulted in a uniform structural response regardless of the loading direction. Additionally, the maximum resistance observed in this configuration, approximately 10 kN, was significantly lower compared to the S1 configuration. This suggests that the investigated connection is more susceptible to shear forces. The increase in stiffness at a displacement of about 60 mm is linked to a change in the stress distribution once the specimen reached a significant deformation, causing the loading direction to lose its perpendicularity with respect to the pipe, thus inducing a tensile component. The analysis was stopped at a displacement of 130 mm due to the substantial yielding of the specimens.

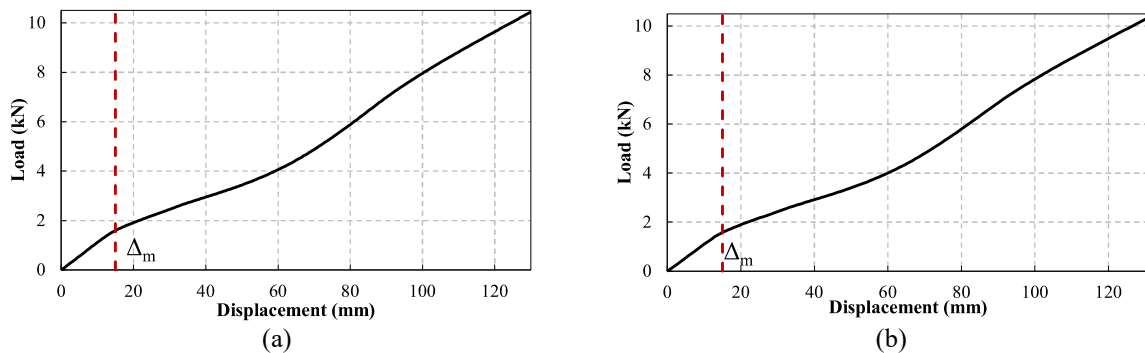


Figure 8: Monotonic load-displacement curves for S2: (a) upward displacement, (b) downward displacement

As shown in Figure 9, the pushover curves for S3 exhibit distinct responses depending on the direction of loading. This discrepancy arises because, although the specimen and applied constraints are initially symmetric, the decomposition of the applied force along the two main directions—parallel and perpendicular to the pipe's longitudinal axis—results in different force distributions. Additionally, similar to specimen S2, as the specimen undergoes increasing deformations, variations in the loading direction relative to the main axes lead to an increase in stiffness when the displacement is applied in the upward direction.

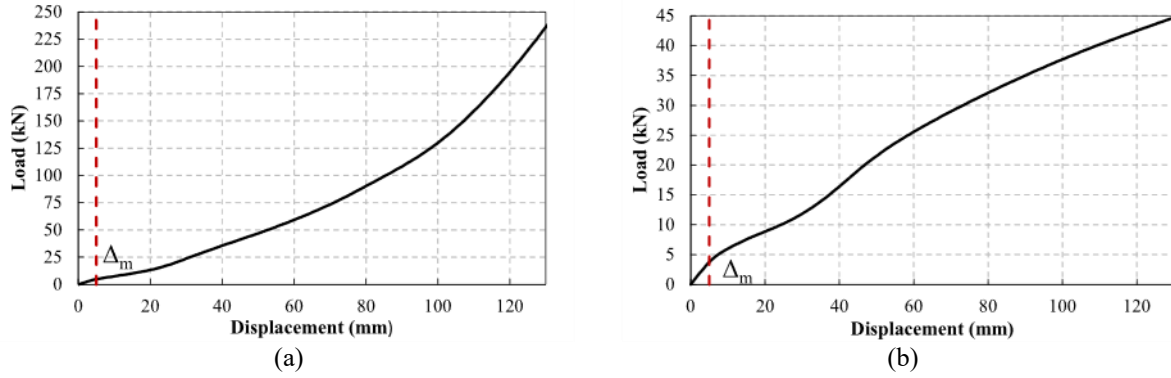


Figure 9: Monotonic load-displacement curves for S3: (a) upward displacement, (b) downward displacement

3.2 Protocols for cyclic testing

The experimental cyclic tests will be conducted under displacement control, following the FEMA-461 cyclic loading protocol for quasi-static testing. The objective of this protocol is to fully characterize the hysteretic response of the tested specimens and to provide performance parameters that are useful for both design purposes and the definition of fragility functions. This loading protocol distinguishes itself from other available protocols for non-structural elements, such as FM-Global [20], by offering a more gradual increase in displacement amplitude, allowing for a detailed study of the nonlinear response propagation. In contrast, other protocols are more suited for investigating fatigue-related issues [21].

According to FEMA-461, the loading history consists of cycles of progressively increasing amplitude. Two cycles are required for each amplitude. Load history is defined by four parameters [19]:

Δ_0 = the targeted smallest deformation amplitude of the loading history

Δ_m = the targeted maximum deformation amplitude of the loading history

n = the number of steps in the loading history, generally 10 or larger

a_i = the amplitude of the cycles, as they increase in magnitude, i.e., the first amplitude, a_1 , is Δ_0 (or a value close to it), and the last planned amplitude, a_n , is Δ_m (or a value close to it).

The following equation gives the amplitude a_{i+1} of step $i+1$:

$$a_{i+1} = 1.4a_i \tag{1}$$

where a_i is the amplitude of the preceding step, and a_n is the amplitude of the step close to the target displacement, Δ_m . If the specimen has not reached the final damage state at Δ_m , the amplitude shall be increased further by the constant increment of $0.3\Delta_m$.

The cyclic loading protocols adopted for the cyclic analyses and for future experimental tests are reported in Figure 10 and Figure 11. For specimen S1, the maximum amplitude was determined by considering the displacement corresponding to a 20% reduction in the maximum force recorded during the monotonic analysis, as shown in Figure 7. Specifically, a maximum amplitude of 40 mm was selected.

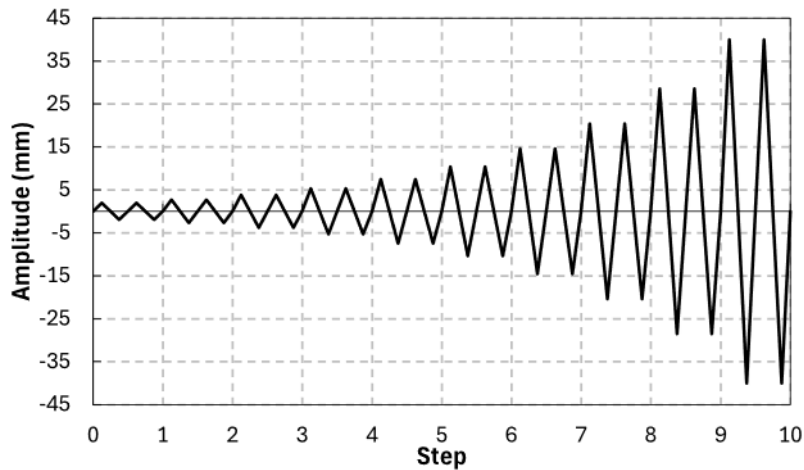


Figure 10: Cyclic loading protocol for S1

Regarding S2 and S3, which did not exhibit a degradation phase during the monotonic analyses, the displacement corresponding to the first plate yielding was considered as target displacement in the definition of the loading protocol; specifically, a displacement equal to 15 mm for S2 and equal to 5 mm for S3 (dotted line in Figure 8 and Figure 9) was considered. In these two cases, since the degradation phase was not achieved, the protocol was extended by additional five cycles with a constant increment of $0.3\Delta_m$, until 37.5 mm for S2 and 12,5 mm for S3 (Figure 11).

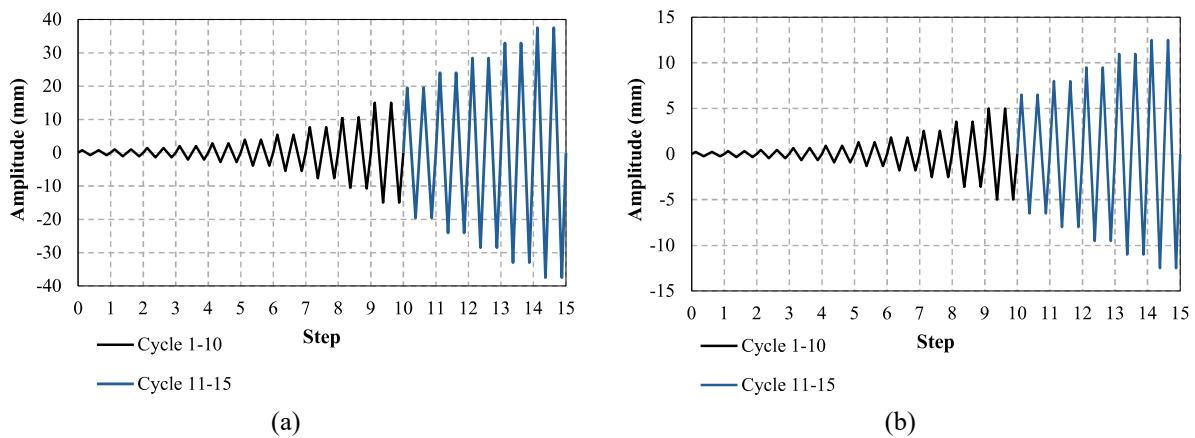


Figure 11: Cyclic loading protocols for: (a) S2, (b) S3

3.3 Numerical simulation of quasi-static cyclic tests

The quasi-static cyclic tests for each specimen were simulated according to the loading protocol defined in Section 3.2. These preliminary analyses aim to predict the experimental behaviour of the specimens and confirm the capability of numerical models to simulate the performance of pipe-to-tank connections.

The hysteretic response of S1 (Figure 12) indicated that, during the tensile phase, the load increased progressively with displacement. In the compressive phase, the maximum load attained was approximately equal to 90 kN. This load was slightly lower than that observed in monotonic analyses, likely due to the degradation effects induced by cyclic loading, which may have contributed to a reduction in the specimen's strength.

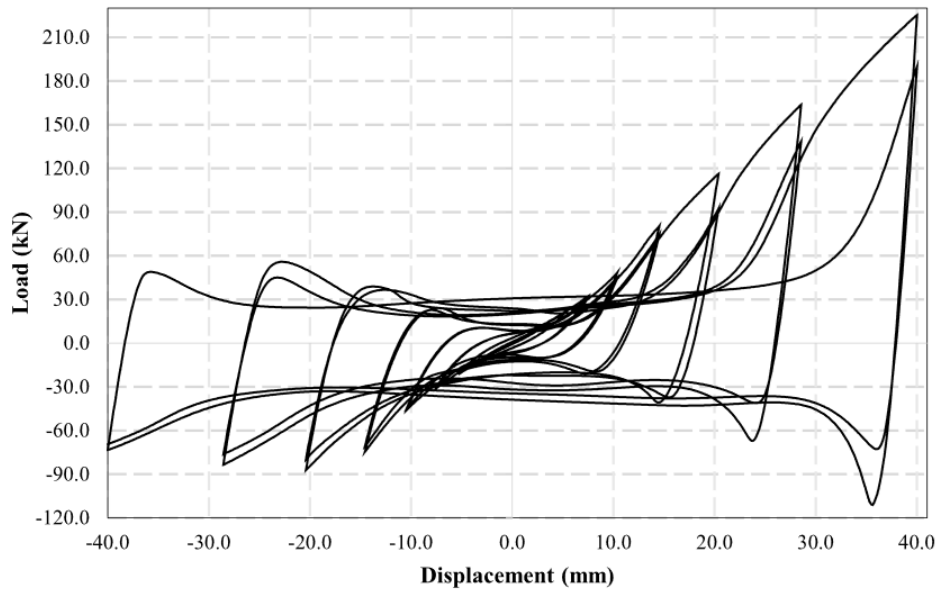


Figure 12: Cyclic load-displacement curves of S1

The hysteretic curves obtained for S2 and S3 (Figure 13) confirmed the results obtained during the pushover analyses. In general, specimen S2, which was subjected to a shear load, is characterized by a lower capacity. In both cases, regular cyclic loops were observed without pinching effects and degradation phases. The maximum load achieved at the target displacements was equal to 2.8 kN and 8 kN, respectively, for S2 and S3.

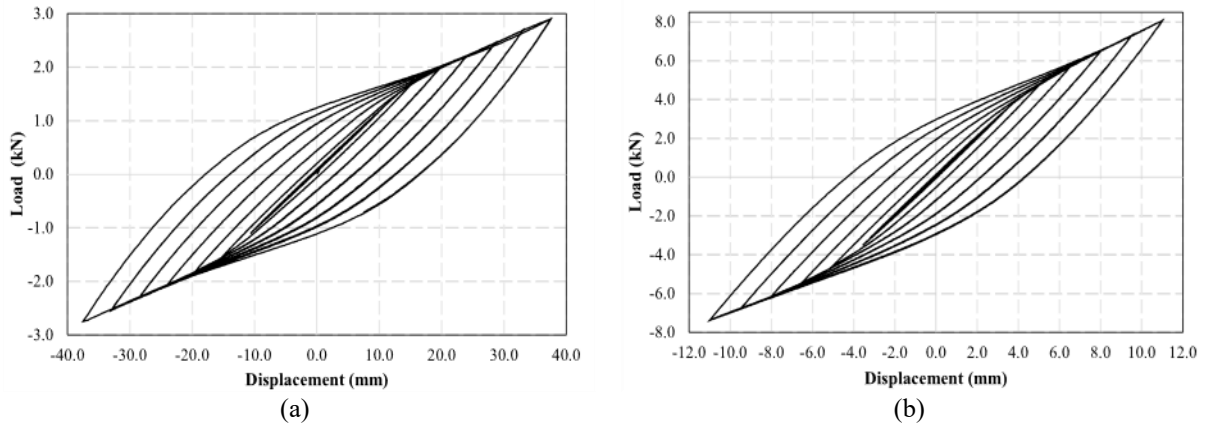


Figure 13: Cyclic load-displacement curves: (a) S2, (b) S3

Figure 14 presents the stress distribution in S1 at a displacement equal to 7.44 mm and 40 mm. Yielding first occurred in the shell plate at its connection with the pipe, while at a displacement equal to 40 mm, the pipe itself reached its yield strength.

Figure 15 shows the stress states for S2 and S3 at the maximum displacement achieved during the numerical analyses (37.5 mm and 12.5 mm, respectively); in both cases, the shell plate attained its yield strength.

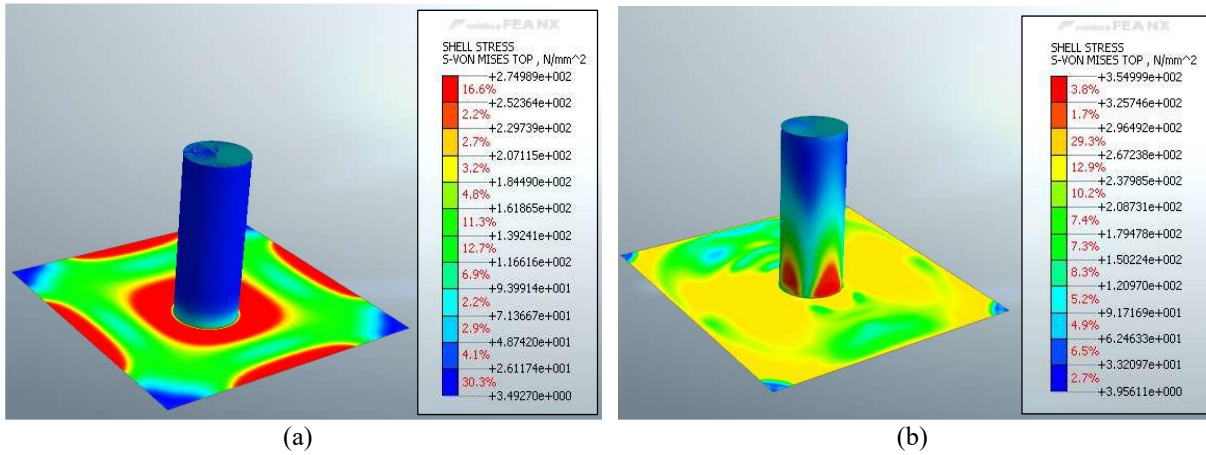


Figure 14: Stress states of S1 at displacement of 7.44 mm (a) and 40 mm (b)

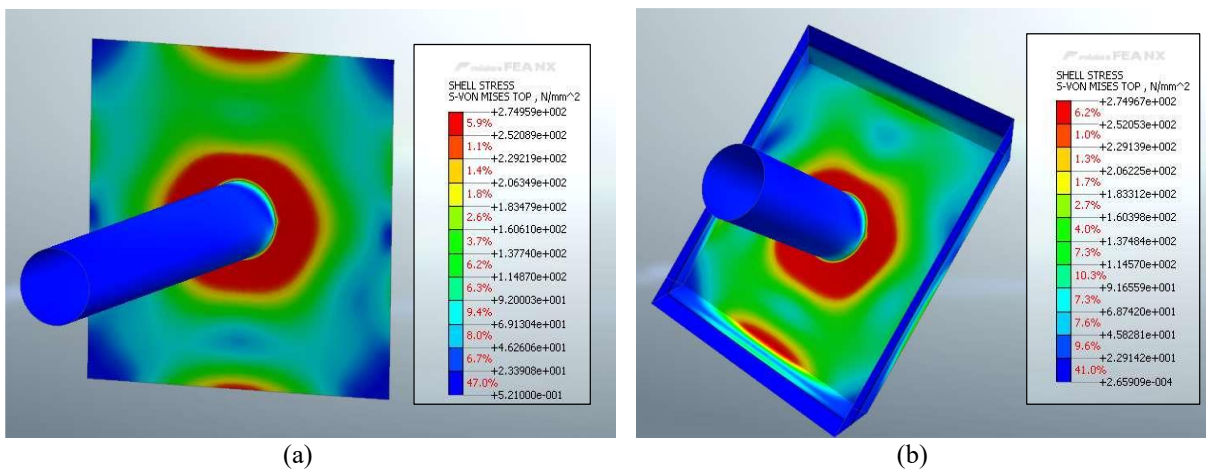


Figure 15: Stress states of: S2 at a displacement of 37.5 mm (a) and S3 at a displacement of 12.5 mm (b)

4 CONCLUSIONS

Pipe-to-tank connections are particularly susceptible to seismic events, making their vulnerability a critical factor in the seismic assessment of industrial plants.

In this study, preliminary quasi-static monotonic and cyclic numerical analyses on pipe-to-tank connections subjected to three different loading conditions were presented. The numerical models are aimed at predicting the response of experimental tests that will be carried out in the near future. The results of the quasi-static monotonic and cyclic analyses revealed an increased structural capacity under tensile stresses and a reduction in strength under compressive and pure shear loading conditions. The nonlinear response is mainly related to the yielding of the steel plate close to the connection to the pipe, demonstrating the importance of adequately creating the pipe-to-tank connection.

The results of the experimental campaign will provide valuable insights into the failure modes of connections, and they will support the recalibration of the numerical models for future parametric analyses. Furthermore, this research will contribute to assessing whether pipe-to-tank connections, designed for static loads according to EN 14015, also demonstrate adequate seismic performance.

REFERENCES

- [1] M. Campedel, Analysis of major industrial accidents triggered by natural events reported in the principal available chemical accident databases, *JRC Scientific and Technical Reports*, JRC42281, 2008.
- [2] F. Paolacci, R. Giannini, M. De Angelis, M. Ciucci, Seismic vulnerability of major-hazard industrial plants and applicability of innovative seismic protection systems for its reduction, *11th World Conference on Seismic Isolation, Energy Dissipation and Active Vibration Control of Structures*, Guangzhou, China, 2009.
- [3] G. Gabbianelli, D. Perrone, F. Micelli, M. Ciucci, Damage evaluation and mitigation in industrial facilities due to natech seismic events, *18th world conference on earthquake engineering*, Milan, 2024.
- [4] M. Ciucci, L. Barbieri Vita, A. Marino, Rischio NaTech da sisma negli stabilimenti con Pericolo di Incidente Rilevante: metodologie di valutazione e gestione, *SAFAP*, 2021.
- [5] M. Salimbeni, M. De Angelis, M. Ciucci, Earthquake NaTech risk assessment in major-hazard industrial plants, a case study: cylindrical liquid storage tank with floating roof, *Chem. Eng. Trans.*, 91, 193-198, 2022.
- [6] M. Vathi, S. Karamanos, I.A. Kapogiannis, K.V.Spiliopoulos, Performance Criteria for Liquid Storage Tanks and Piping Systems Subjected to Seismic Loading, *Journal of Pressure Vessel Technology*, 2017.
- [7] EN 1998-4, Eurocode 8: Design of structures for earthquake resistance – Part 4: Silos, tanks and pipelines, 2006.
- [8] EN 14015, Specification for the design and manufacture of site built, vertical, cylindrical, flat-bottomed, above ground, welded, steel tanks for the storage liquids at ambient temperature and above, 2006.
- [9] API STANDARD 650, Welded tanks for oil storage, 2021.
- [10] API STANDARDS 620, Design and construction of large, welded, low-pressure storage tanks, 2018.
- [11] M. Pantusheva, Seismic analyses of steel storage tanks: overview of design codes used in practice, *International Jubilee Scientific Conference “75th Anniversary of UACEG” University of architecture, civil engineering and geodesy*, November 1-3, 2017.
- [12] M. S. Reza, O. S. Bursi, F. Paolacci, A. Kumar, Enhanced seismic performance of non-standard bolted flange joints for petrochemical piping systems, *Journal of Loss Prevention in the Process Industries*, 2014.
- [13] V. La Salandra, O. S. Bursi, S. Alessandri, R. Di Filippo, F. Paolacci, Cyclic response of enhanced bolted flange joints for piping systems, *Proceedings of the ASME 2016 Pressure Vessels & Piping Conference*, Vancouver, British Columbia, Canada, July 17-21, 2016.
- [14] G. E. Varelis, J. Ferino, S. A. Karamanos, A. Lucci, G. Demonti, Experimental and numerical investigation of pressurized pipe elbows under strong cyclic investigation, *Proceedings of the ASME 2013 Pressure Vessels and Piping Conference*, PVP 3013, Paris, France, July 14-18, 2013.

- [15] T. Papatheocharis, K. Diamanti, G. E. Varelis, P. C. Perdikaris, S. A. Karamanos, *Proceedings of the ASME 2013 Pressure Vessels and Piping Conference*, PVP2013, July 14-18, Paris, France, 2013.
- [16] M. Aiba, K. I. Grashi, H. Akiyama, T. Chiba, Test of nozzles at wall of cylindrical tank for severe loads under earthquake, *12th World Conference on Earthquake Engineering*, Paper No. 2586, Auckland, New Zealand, 2000.
- [17] M. Wieschollek, B. Hoffmeister, M. Feldmann, Experimental and numerical investigations on nozzle reinforcements, *Proceedings of the ASME 2013 Pressure Vessels and Piping Conference*, PVP2013, July 14-18, Paris, France, 2013.
- [18] R. Manshoori, Evaluation of Seismic Vulnerability and Failure Modes for Pipelines, *Procedia Engineering*, 14, 3042-3049, 2011.
- [19] FEMA 461, Interim Testing Protocols for Determining the Seismic Characteristics of Structural and Nonstructural Components, 2007.
- [20] FM Approvals LLC, Approval Standard for Seismic Sway Braces for Automatic Sprinkler Systems, FM Global Group, Norwood, MA 02062, USA, p. 25, 2010.
- [21] A. Filiatrault, D. Perrone, E. Brunesi, C. Beiter, R. Piccinin, Effect of cyclic loading protocols on the experimental seismic performance evaluation of suspended piping restraint installations, *International journal of pressure vessels and piping*, 166:61-71 <https://doi.org/10.1016/j.ijpvp.2018.08.004>, 2018.